

# Improved Dark Energy Detection through the Polarization-assisted WMAP-NVSS ISW Correlation

Guo-Chin, Liu<sup>1</sup>, Kin-Wang, Ng<sup>2,3</sup>, and Ue-Li, Pen<sup>4</sup>

October 5, 2010

<sup>1</sup>*Department of Physics, Tamkang University, 251-37 Tamsui, Taipei County, Taiwan 251, R.O.C.*

<sup>2</sup>*Institute of Astronomy and Astrophysics, Academia Sinica, Taipei, Taiwan 115, R.O.C.*

<sup>3</sup>*Institute of Physics, Academia Sinica, Taipei, Taiwan 115, R.O.C.*

<sup>4</sup>*Canadian Institute for Theoretical Astrophysics, University of Toronto, 60 St. George Street, Toronto, ON M5S 3H8, Canada*

## Abstract

Integrated Sachs-Wolfe (ISW) effect can be estimated by cross-correlating Cosmic Microwave Background (CMB) sky with tracers of the local matter distribution. At late cosmic time, the dark energy induced decay of gravitation potential generates a cross-correlation signal on large angular scales. The dominant noise are the intrinsic CMB anisotropies from the inflationary epoch. In this *Letter* we use CMB polarization to reduce this intrinsic noise. We cross-correlate the microwave sky observed by Wilkinson Microwave Anisotropy Probe (WMAP) with the radio source catalog compiled by NRAO VLA Sky Survey (NVSS) to study the efficiency of the noise suppression. We find that the error bars are reduced about 5 – 12%, improving the statistical power.

Recently released data made by Wilkinson Microwave Background Probe (WMAP) [1] is used to study different cosmological models with an unprecedented accuracy. The observed data puts tight constraints on intrinsic properties of the Universe such as the geometry, the matter content, the origin

of inhomogeneities, and the formation of large scale structures. Furthermore, combining observations from type Ia supernovae [2] and large scale structures (e.g. Allen et al. 2002 [3]) converges our understanding of the Universe to a concordance model. In this model, the present Universe is dominated by dark energy with negative pressure which is accelerating at late times. Although dark energy can explain the acceleration, we know very little about its nature and origin. More observations are definitely necessary for constraining this dark energy component.

As CMB photons propagate through a gravitational potential generated by large scale structures in the expanding Universe, the photons undergo an energy shift. In a matter-dominated universe, the gravitational potential stays a constant, so the CMB temperature fluctuations generated through this so-called Sachs-Wolfe (SW) effect [4] depend only on the potential difference between the recombination epoch and the present time. However, the existence of a spatial curvature or dark energy results in a time-varying gravitational potential, thus producing, in addition to the SW effect, time-integrated temperature fluctuations of the CMB. This is known as the integrated Sachs-Wolfe (ISW) effect [4]. Therefore, the detection of the late-time ISW effect in a flat universe can be regarded as direct dynamical evidence for dark energy. Furthermore, measuring the ISW effect provides an independent method to probe the properties of dark energy.

The ISW effect manifests itself on large angular scales because the CMB temperature fluctuations or anisotropies are dominantly induced by the gravitational potential at large scales. On these angular scales, the CMB signal is dominated by the primary anisotropies generated from the recombination epoch at redshift  $z \simeq 1100$  as well as from the reionization epoch at redshift  $z \simeq 10$ . It is not easy to isolate the ISW effect from the primary CMB fluctuations. The precision of large-scale anisotropy power measurement is limited by the unavoidable cosmic variance. Therefore, attempts in measuring the ISW effect solely from CMB experiments may not be able to give tight constraints on dark energy models.

However, a positive large-scale correlation signal may occur by correlating the CMB sky with the local matter distribution as a result of the ISW effect. This idea was first explored by Crittenden and Turok (1996). Several authors tried to detect the ISW effect by correlating CMB satellite data with different matter tracers. The CMB anisotropy data made by the COsmic Background Explorer (COBE) was firstly used for this study [5]. But the authors concluded that the resolution and sensitivity of COBE were not good enough for a detection. Recently, the WMAP mission has

provided a set of high-quality CMB data. As to the matter distribution, several tracers have been used for this study, such as radio sources provided by NRAO VLA Sky Survey (NVSS) [6], hard X-ray data from High Energy Astronomy Observatory-1 satellite (HEAO-1) [7], Sloan Digital Sky Survey (SDSS) data [8], and Two Micron All Sky Survey Extended Source Catalog (2MASS XSC) [9]. Douspis et al. 2008 [10] has investigated the properties of a survey required to detect this correlated signal. The data analyses of the cross-correlation are performed in real [5, 11, 12], harmonic [13], and wavelet [14, 15] spaces.

A significant uncertainty in the cross-correlation is coming from the spurious correlation of matter distribution with the primary CMB anisotropies generated from the recombination and reionization epochs. It plays a role like the cosmic variance in observations of the low multipoles of the CMB anisotropy that have only a few independent modes. This spurious correlation obscures the measurement of the true correlation that we are interested in and indeed weakens the constraint on the dark energy component. However, CMB polarization is also generated when the primary anisotropies are scattered by free electrons in these two epochs. Using the fact that the ISW effect occurs at relatively late times, the information imprinted on the CMB polarization may give an opportunity to separate the ISW effect from the primary anisotropies. If this can be done, we will suppress or even get rid of the spurious correlation. In this *Letter*, we construct a simple relation between the CMB polarization and its corresponding primary anisotropies. This relation is found to be weakly dependent on the emerging dark energy at late times, thus allowing us to subtract the primary CMB anisotropies from the CMB anisotropy data to obtain the genuine ISW signal. Then, the resulting anisotropies are used to correlate with matter tracers to obtain a better signal-to-noise detection of the cross-correlation.

Instead of using Stokes parameters  $Q$  and  $U$  [16], CMB polarization is conventionally characterized by a divergence free component, commonly called the  $E$  mode, and a curl component, the  $B$  mode. Small-scale polarization of the CMB is generated through Thomson scattering of the CMB anisotropic radiation by free electrons at the recombination epoch. For the angular scales at which the cross-correlated ISW effect is concerned,  $E$ -mode polarization is generated by re-scattering off the free electrons at reionization epoch, and  $B$ -mode polarization is also generated in the presence of tensor-mode perturbations, predicted for example in inflation model. So far, there is no evidence for the  $B$  mode polarization, so we will not consider it.

Since CMB polarization is generated from temperature anisotropies, we expect some relation between the  $E$ -mode polarization and the CMB anisotropies. We simply assume that the relation can be written as

$$E_\ell^{\text{NOISW}} = a_\ell T_\ell^{\text{NOISW}} + n_\ell. \quad (1)$$

Here  $E_\ell^{\text{NOISW}}$  and  $T_\ell^{\text{NOISW}}$  are the  $E$ -mode polarization and temperature anisotropies in each multipole  $\ell$ , each coefficient  $a_\ell$  quantifies the amount of the correlation between the  $E$ -mode polarization and the temperature anisotropies, and  $n_\ell$  plays a role like the “noise” of this relation. For our purpose, we construct this relation in the situation in which the ISW effect is removed.

We define the “ $E$ -mode polarization corrected” temperature anisotropies as

$$\tilde{T}_\ell^{\text{E-COR}} = T_\ell - E_\ell/a_\ell \simeq T_\ell - E_\ell^{\text{NOISW}}/a_\ell. \quad (2)$$

We have made the approximation in the last equality due to the fact [17, 18] that the polarization contributed by the ISW effect is significantly smaller than that by the primary temperature quadrupole re-scattering at the reionization. Then, we cross-correlate  $E_\ell^{\text{NOISW}}$  in equation (1) with the CMB temperature anisotropies:

$$\langle TE \rangle_\ell^{\text{NOISW}} = a_\ell \langle TT \rangle_\ell^{\text{NOISW}}, \quad (3)$$

and obtain the auto-correlation as

$$\langle EE \rangle_\ell^{\text{NOISW}} = a_\ell^2 \langle TT \rangle_\ell^{\text{NOISW}} + n_\ell^2. \quad (4)$$

Thus, we can calculate the sets  $a_\ell$  and  $n_\ell$  using equations (3) and (4), given the power spectra  $C_{T\ell}$ ,  $C_{C\ell}$ , and  $C_{E\ell}$  from the theoretical prediction. Once the two sets are determined, they can be applied to real data. However, in numerical practice, we have found that the numbers of  $a_\ell$  are quite small and the noise term  $n_\ell^2$  is in fact comparable to  $\langle EE \rangle_\ell$ . It means that  $T_\ell - E_\ell/a_\ell$  may result in an over subtraction due to the noise  $n_\ell$ . To circumvent this problem, we multiply each  $E_\ell/a_\ell$  by a Wiener filter constructed as

$$W_{1\ell} = \langle TT \rangle_\ell / (\langle TT \rangle_\ell + n_\ell^2/a_\ell^2). \quad (5)$$

In Fig. 1, we plot the  $E$ -mode polarization corrected power spectrum (denoted by the dot-dashed curve) of the temperature anisotropies,  $\langle \tilde{T} \tilde{T} \rangle_\ell^{\text{E-COR}}$ , where  $\tilde{T}_\ell^{\text{E-COR}}$  is defined in equation (2). In determining  $a_\ell$  and  $n_\ell$ , we have

generated 500 CMB sky maps, using the power spectra obtained from running the CMBFast code [19] with the WMAP best-fit cosmological parameters. For the necessary power spectra used in equations (3) and (4), we have removed the ISW effect in the CMBFast code by forcing the time-varying gravitational potential to vanish for redshift  $z < 5$ . For the comparison, we also plot the total power spectrum of the temperature anisotropies and the isolated ISW effect, respectively denoted by the solid and the dashed curves. We have found that we can filter out more than about 10% of the primary temperature anisotropies for the multipoles  $\ell < 30$ . For  $40 < \ell < 70$ , the correction is inefficient due to the low  $\langle TE \rangle$  correlation from the theoretical prediction. More efficient correction occurs for  $80 < \ell < 100$  (in Fig. 1); however, the cross-correlation signal of the CMB and large-scale-structure is small at this angular scale [20].

Now we apply the “corrected” temperature anisotropies described above to calculate its cross-correlation with the matter tracers. We use the WMAP 7-year foreground reduced maps with full resolution. We take only the Q and V frequency channels because of the low contamination of the foreground emission on both temperature anisotropies and polarization [1]. For the matter distribution, we use NVSS radio sources. NVSS is operated at 1.4 GHz with flux limit 2.5 mJy. It is complete for declination  $\delta > -40^\circ$  and contains 1.8 million sources. Its 82% sky coverage provides good information at large angular scales. Though the redshifts of individual radio sources are largely unknown, the luminosity function [21] indicates that they are distributed in redshift range  $0 < z < 2$ , with a peak distribution at  $z \sim 0.8$ . Crittenden and Turok (1996) have studied the signal contribution of the cross-correlation with different cutoffs in redshift [20] and concluded that the redshift distribution of the NVSS radio sources is very suitable for this study. The cross-correlation power spectrum between NVSS and WMAP is simply calculated by

$$C_\ell^{NW} = \frac{1}{2\ell + 1} \sum_m \langle a_{\ell m}^N a_{\ell m}^{*W} \rangle, \quad (6)$$

where  $a_{\ell m}^N$  and  $a_{\ell m}^W$  are the harmonic coefficients of the NVSS and WMAP maps, respectively. We distribute the NVSS catalog in the Healpix scheme [22] at resolution-9 map, whose resolution is the same with the WMAP 7-year foreground reduced maps. Such map has  $12N_{side}$  pixels with the same area in all sky, where  $N_{side} = 2^9$ . We calculate the coefficients of the spherical harmonics  $a_{\ell m}$  for the temperature anisotropies, the  $E$  mode polarization, as well as the NVSS sources, using the Healpix package with a mask which

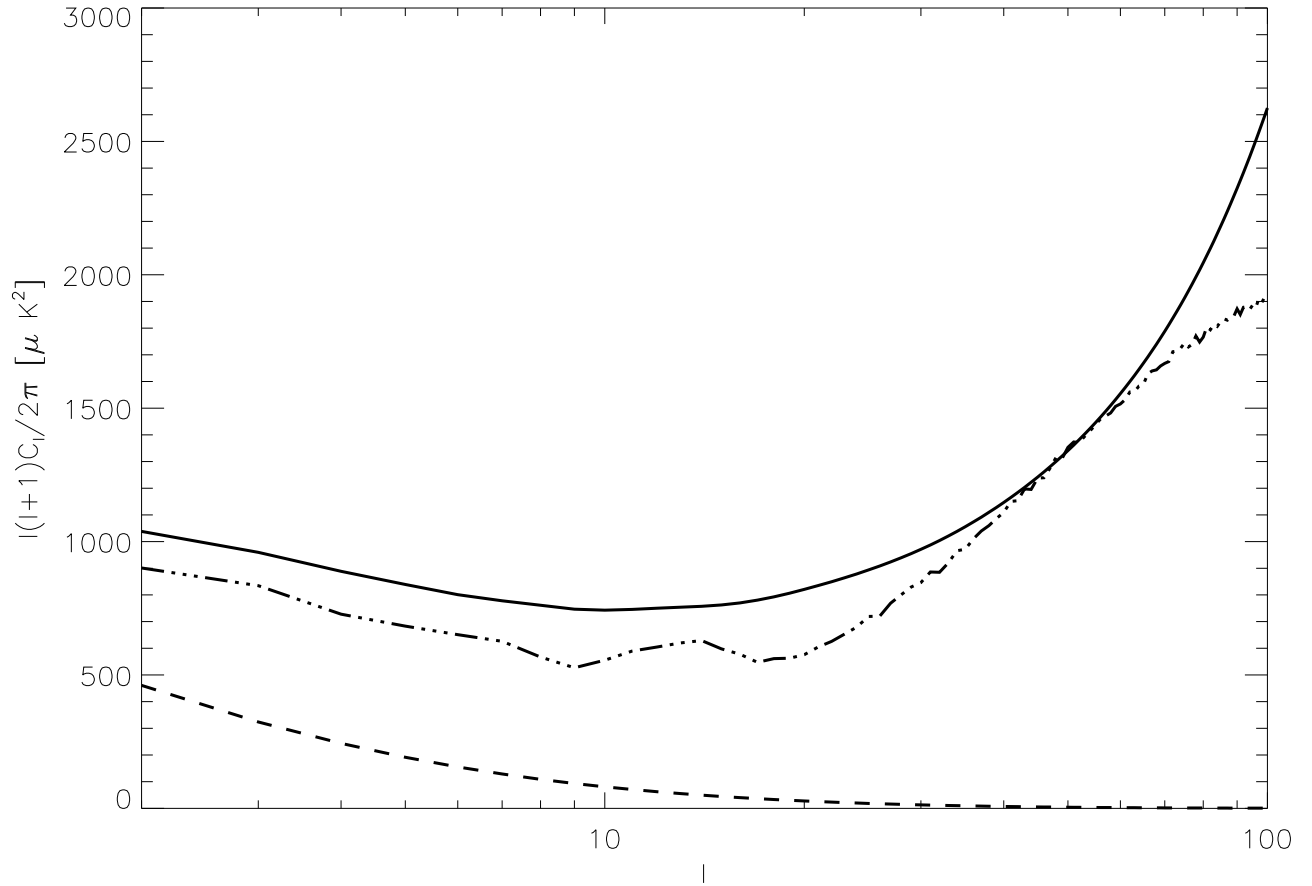


Figure 1: Power spectrum of the CMB temperature anisotropies after the correction by the  $E$ -mode polarization (dot-dashed curve). For comparison, we also plot the total power spectrum before correction (solid curve) and the ISW effect (dashed curve). Using information of  $\langle TE \rangle$  correlation, we can filter out the part of the signal coming from redshifts before  $z = 5$ .

is obtained by combining the standard polarization mask (P06) used by the WMAP team and the blank sky of the NVSS survey. Applying this mask gives a sky coverage of about 56% and the average number density of NVSS radio galaxies is 171494/*sr*.

In Fig. 2, we plot the signal of the cross-correlation of WMAP and NVSS for the Q and V frequency bands. To reduce the correlation among neighboring multipoles, we bin our results into five bins with equal spaces in logarithm- $\ell$  from 2 to 100 (We found that masking about 44% of the sky would cause about 44% correlation among neighboring multipoles). The instrumental noise in the WMAP data at such large angular scales is negligible when compared to temperature anisotropies, but it is comparable to the  $E$  polarization signal. Therefore, in practice, we find the *estimated* ISW temperature as

$$\tilde{T}_\ell^{\text{E-COR}} = T_\ell - W_{1\ell}W_{2\ell}E_\ell^{\text{NOISW}}/a_\ell, \quad (7)$$

with one more Wiener filter given by

$$W_{2\ell} = \langle EE \rangle_\ell / (\langle EE \rangle_\ell + N_\ell), \quad (8)$$

where  $N$  is the covariance matrix for the instrumental noise. We have calculated  $N$  by the thermal noise in each pixel provided by WMAP team without taking into account the correlated noise between different pixels. It may cause the wrong power estimation in low- $\ell$  multipoles. We also need to notice that we cannot obtain the exact values of the multipoles by this method due to the incomplete coverage of the sky. In case of modelling or parameter fitting, we need to estimate these two factors carefully.

The spurious correlation resulted from the primary CMB temperature anisotropies can be quantified using simulated, uncorrelated CMB maps. We use the 500 simulated CMB sky maps in the previous section to do the blind correlation with the real NVSS data. The error bars in Fig. 2 show the  $1\sigma$  region derived from this result. Let us define  $\chi^2 = \sum_i (\hat{C}_{Bi} - C_{Bi})^2 / \sigma_{Bi}^2$ , where  $\hat{C}_{Bi}$  and  $C_{Bi}$  are respectively the measured and predicted band powers of the WMAP-NVSS cross-correlation, and  $\sigma_{Bi}$  is the  $1\sigma$  error of the  $i$ th band. For a model with null correlation, i.e.,  $C_{Bi} = 0$ , we find that  $\chi^2 = 9.8$  for the Q band and  $\chi^2 = 9.0$  for the V band in the case without the  $E$ -polarization correction. After the  $E$ -polarization correction, the values increase to  $\chi^2 = 11.7$  for the Q band and  $\chi^2 = 10.6$  for the V band. We also find that the correction improves the errors resulted from the spurious correlation by 6.0%, 9.5%, 12.3%, 4.9%, and 7.3% in the five respective bins.

We acknowledge the extensive use we have made of data from the WMAP satellite, and thank Dr. L. Chiang for fruitful discussions on the WMAP data. We also appreciate discussions with Drs. N. Aghanim and M. Douspis. G.-C. Liu (K.-W. Ng) thanks for the support from the National Science Council of Taiwan under the grant NSC97-2112-M-032-007-MY3 (NSC98-2112-M-001-009-MY3) and support from the Institute of Physics, Academia Sinica.

## References

- [1] Jaroski, N., et al. 2010, *Astrophysical Journal Supplement Series*, submitted
- [2] Knop, R. A., et al. 2003, *ApJ*, 598, 102
- [3] Allen, S. W., Schmidt, R. W. & Fabian, A. C., 2002, *Mon. Not. R. Astron. Soc.*, 334, 11
- [4] Sachs, R. K., & Wolfe, A. M. 1967, *ApJ*, 147, 73
- [5] Boughn, S. P., & Crittenden, R. G., 2002, *Phys. Rev. Lett.*, 88, 021302
- [6] Condon, J. J., Cotton, W. D., Greisen, E. W., Yin, Q. F., Perley, R. A., Taylor, G. B., & Broderick, J. J. 1998, *ApJ*, 115, 1693
- [7] Boldt, E. 1987, *Phys. Rep.*, 146, 215
- [8] York, D. G., et al. 2000, *Astron. J.*, 120, 1579
- [9] Jarrett, T. H., Chester, T., Cutri, R., Schneider, S., Skrutskie, M., & Huchra, J. P. 2000, *Astron. J.*, 119, 2498
- [10] Douspis, M., Castro, P. G., Caprini, C., & Aghanim, N. 2008, *A&A*, 485, 395
- [11] Boughn, S. P., & Crittenden, R. G. 2004, *Nature*, 427, 45
- [12] Nolta, M. R., et al. 2004, *ApJ*, 517, 565
- [13] Afshordi, N., Loh, Y. S., & Strass, M. A. 2004, *Phys. Rev. D*, 69, 083542
- [14] Vielva, P., Martinez-Gonzalez, E., & Tucci, M. 2006, *Mon. Not. R. Astron. Soc.*, 365, 891



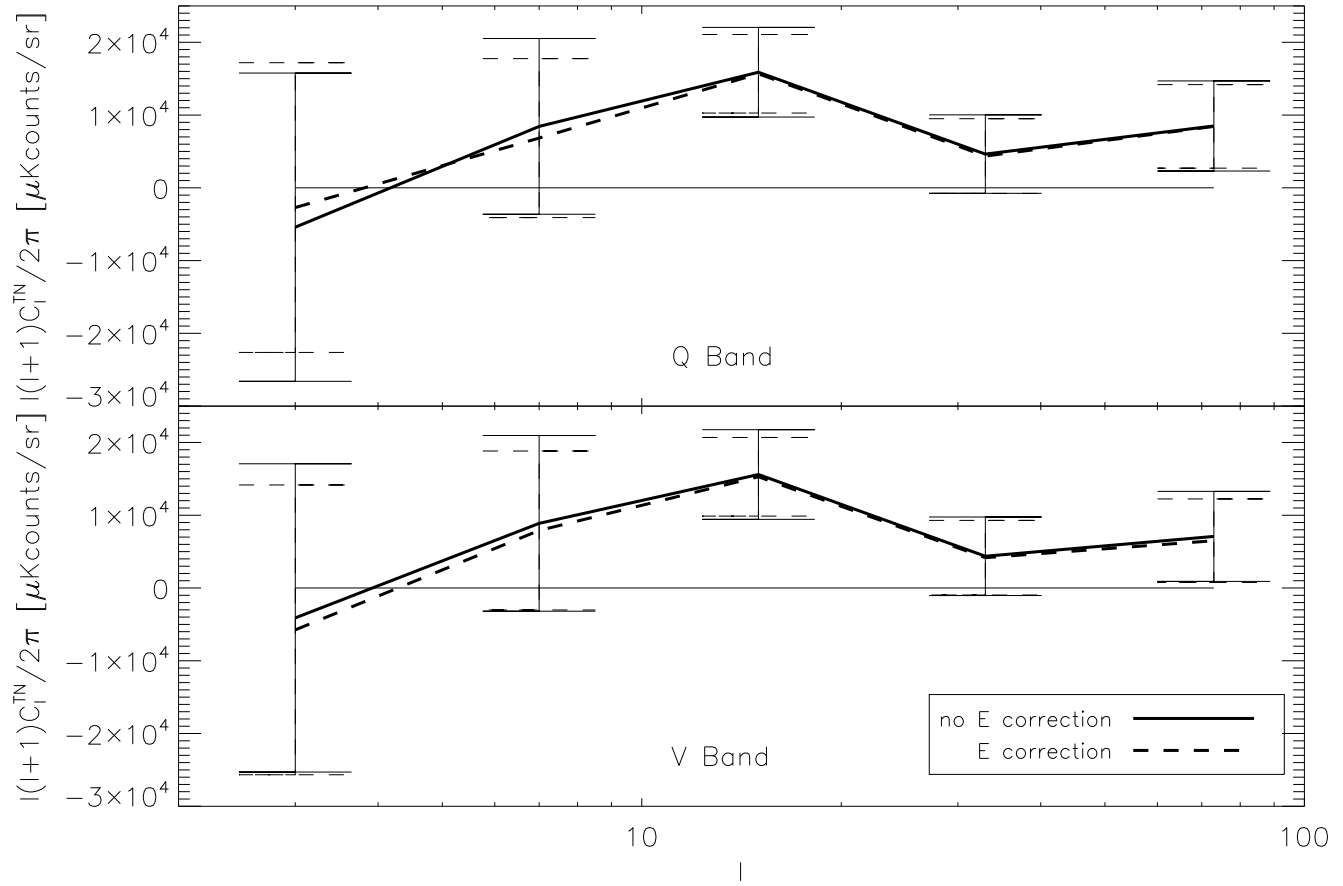


Figure 2: Cross-correlation of WMAP and NVSS for Q and V frequency bands. The errors bars are calculated by cross-correlated 500 simulated CMB skys with NVSS catalog. Using  $E$ -polarization, the error bars and signal of cross-correlation are changed.

- [15] McEwen, J. D., Wiaux, Y., Hobson, M. P., Vandergheynst, P., & Lasenby, A. N. 2008, *Mon. Not. R. Astron. Soc.*, 384, 1289
- [16] Chandrasekar, S. 1960, *Radiative Transfer* (Dover, New York, 1960)
- [17] Ng, K.-W. 1996, in *Proc. of the 1st RESCEU Int. Symp., Cosmological Constant and the Evolution of the Universe*, ed. K. Sato, T. Sugihara, & N. Sugiyama (Universal Academy Press), 31
- [18] Cooray, A. & Melchiorri, A. 2006, *JCAP*, 01, 018C
- [19] Seljak, U., & Zaldarriaga, M. 1996, *ApJ*, 469, 437
- [20] Crittenden, R. G., & Turok, N. 1996, *Phys. Rev. Lett.*, 76, 575
- [21] Dunlop, J. S., & Peacock, J. A. 1990, *Mon. Not. R. Astron. Soc.*, 247, 19
- [22] Gorski, K. M., Hivon, E., Banday, A. J., Wandelt, B. D., Hansen, F. K., Reinecke, M., & Bartelmann, M. 2005, *ApJ*, 622, 759